Assessing The Importance Of Colours For CNNs In Object Recognition

Aditya Singh, Alessandro Bay, Andrea Mirabile
Zebra AI, Zebra Technologies
London, United Kingdom
{firstname.lastname}@zebra.com

Abstract

Humans rely heavily on shapes as a primary cue for object recognition. As secondary cues, colours and textures are also beneficial in this regard. Convolutional neural networks (CNNs), an imitation of biological neural networks, have been shown to exhibit conflicting properties. Some studies indicate that CNNs are biased towards textures whereas, another set of studies suggests shape bias for a classification task. However, they do not discuss the role of colours, implying its possible humble role in the task of object recognition. In this paper, we empirically investigate the importance of colours in object recognition for CNNs. We are able to demonstrate that CNNs often rely heavily on colour information while making a prediction. Our results show that the degree of dependency on colours tend to vary from one dataset to another. Moreover, networks tend to rely more on colours if trained from scratch. Pre-training can allow the model to be less colour dependent. To facilitate these findings, we follow the framework often deployed in understanding role of colours in object recognition for humans. We evaluate a model trained with congruent images (images in original colours eg. red strawberries) on congruent, greyscale, and incongruent images (images in unnatural colours eg. blue strawberries). We measure and analyse network's predictive performance (top-1 accuracy) under these different stylisations. We utilise standard datasets of supervised image classification and fine-grained image classification in our experiments.

1 Introduction

Colours play a vital role in our day to day life. We utilise colours for visual identification [1], search [2], gaze guidance in natural scenes [3] etc. As an example, importance of colour can be understood whilst identifying ripe fruits in a background of foliage [1]. Initially, it was widely believed that only shapes and not colours influence object recognition in humans [4, 5]. However, many studies [6, 7] indicate that colours do assist object recognition in humans. The findings by Tanaka and Presnell [6] show that colours facilitate recognition of high colour diagnostic objects (natural objects like fruits) but have little effect on low colour diagnostic objects (man-made objects like airplanes). Their experiments were based on a variation of Stroop effect [8]. Human participants were asked to name objects in different colour schemes. They observed that naming of objects with congruent colours was much faster than naming incongruently coloured objects. Greyscale images served as a neutral medium and the response time for them were in between congruent and incongruent images. In a similar study conducted by Hagen et al. [9] for investigating the role of colour in expert object recognition, similar findings were reported. Neural networks are models of machine learning designed to mimic the neurological working of a human brain [12]. Today, they are employed in many different fields solving numerous tasks [13–15]. Considering the widespread adoption and blackbox nature of neural networks, considerable studies have also been performed to understand their inner working

2nd Workshop on Shared Visual Representations in Human and Machine Intelligence (SVRHM), NeurIPS 2020.

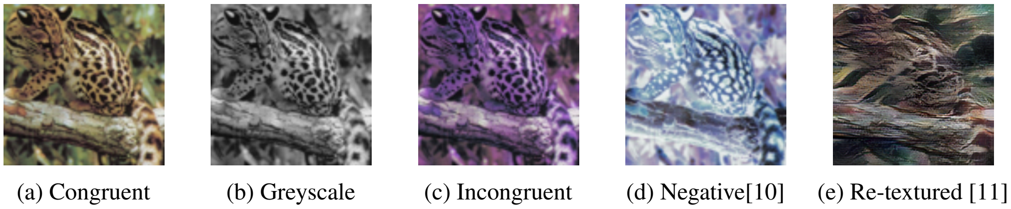

(a) Congruent (b) Greyscale (c) Incongruent (d) Negative[10] (e) Re-textured [11]

Figure 1: The texture and shape information is intact in original, greyscale and incongruent images. Additionally, negative images have a larger drift in distribution than incongruent images when measured against congruent images.

[16–19]. Zeiler and Fergus [16] illustrated the hierarchical nature of learnt features. Engilberge et al. [20] investigated the colour sensitivity of neural networks and observed that at the shallow end the neurons are more sensitive to colour information in an image. A number of existing studies highlight the nature of representations learnt by the network however, do so with conflicting results. One set of results shows that neural networks rely predominantly on shapes [21–25]. On the other hand, many more approaches oppose the theory of shape bias in CNNs [26, 10, 27–29]. Rather than primarily relying on shapes, neural network's predictions are guided by the texture information of an image. Texture is referred to as "a function of the spatial variation in pixel intensities" [30, 31]. Gatys et al. [32] showed that a linear classifier based on texture representations of a neural network performs comparable to the original model. Similarly, Geirhos et al. [11] demonstrated that ImageNet [33] trained model is biased towards texture.

The objective of our paper is to help bridging the gap between human perception and artificial intelligence, providing empirical experiments based on classical neuroscience framework to exhaustively investigate the dependency of CNNs on colour information. We believe the majority of existing approaches do highlight representation bias of CNNs but fail to address the role of colours. Bahng et al. [34] tend to the issue of colour bias in their experiments, however, do so with the motivation to learn unbiased representations. Moreover, by either focusing on small number of test images [21, 29] or a single dataset [11, 26] we are unable to observe a bigger picture.

We believe a fair approach of highlighting the importance of colour is by utilising the framework as used by the psychophysical experiments of [1, 6, 9, 35]. We can easily observe the relevance of colours by comparing performances on congruent and greyscale images. Additionally, by comparing the performances on greyscale and incongruent images we will be able to observe the effect of incorrect colour information (see Figure 4 for sample images).

In this paper, we evaluate the importance of colours for numerous datasets under 2 settings:

1. **Local Information** (Section 4.1): Evaluating the importance of colours when a CNN can only tend to small patches in a global shape agnostic manner.
2. **Global Information** (Section 4.2): For this setting, no such restriction is applied on the network and corresponds to standard approach of training a CNN.

Apart from these 2 modes of experimentation, we also evaluate a model under 4 different training schemes to replicate a typical training scenario for a classification task. We train a network (i) from scratch, (ii) with fine-tuning on pre-trained weights, (iii) with colour based augmentations (random hue, saturation, brightness, etc.), and (iv) with incongruent images to reduce colour dependency. We conclude in Section 5.

2 Data

In our study we have employed datasets from image classification and fine-grained visual classification. The datasets used are: • CIFAR-100 [36] • STL-10 [37] • Tiny ImageNet [38] • CUB-200-2011 [39] • Oxford-Flowers [40] • Oxford-IIIT Pets [41]. Table 5 in appendix provides some common statistics of the datasets used.

3 Method

A dataset $\mathcal{D} = \{(x_i, y_i), i = 1, \ldots, N\}$ is composed of images $x_i \in \mathbb{R}^{C\times H\times W}$ and their corresponding labels y_i. $\mathcal{D}^{train}$, $\mathcal{D}^{test}$ denotes the split of the dataset into train and test sets respectively. We convert $\mathcal{D}$ into different colour schemes as described below:

- **Congruent Images** ($\mathcal{D}_C$): These are the images in original colours. All the subsequent transformations described below are applied to $\mathcal{D}_C$.
- **Greyscale Images** ($\mathcal{D}_G$): The congruent images converted into greyscale(luminance) images, $G = 0.29 * r + 0.587 * g + 0.114 * b$. We copy the single channel greyscale image into 3 channels.
- **Incongruent Images** ($\mathcal{D}_I$): The channels of the congruent images are switched to generate unnaturally coloured images. Formally, the default correspondence for colour channels is as $C[0] = red, C[1] = green, C[2] = blue$. We switch the channels such that the new ordering represents $C[0] = green, C[1] = blue, C[2] = red$. The advantage of it is that firstly, it preserves the texture and secondly, the changes in distribution are more contained than approaches deployed by [10, 11]. For example, the Jensen-Shannon divergence [42] $JS(\mathcal{D}_C^{train}, \mathcal{D}_G^{train}) = 0.06$ and $JS(\mathcal{D}_C^{train}, \mathcal{D}_I^{train}) = 0.1$, whereas same for negative images (as in [10]) and $\mathcal{D}_C^{train}$ is 0.3 for STL-10 dataset. More comparison is provided in appendix A.2.

Figure 4 shows an example of these stylisations. As humans, we learn from our surroundings which we perceive in congruent colours. Since we are following the framework used in identifying role of colours in humans, we train CNNs only on congruent images ($\mathcal{D}_C^{train}$) while evaluating the top-1 accuracy (represented as *Acc*) on the test sets of different stylisations described above.

4 Experiments

4.1 Access to local information

Baker et al. [29] report that CNNs can represent local shapes however, fail to utilise it in a global context. Similarly, to highlight absence of shape bias in a CNN, Geirhos et al. [11] utilise BagNets[28] to compare model performance under artistic stylisations. BagNets only have access to small patches within an image due to its design and utilises bag-of-features based framework for making a prediction. It does not make use of spatial ordering of the local features hence making it suitable to compare the relevance of colours to local shape and texture information.

We use BagNet-9[1] which has a 9 × 9 receptive field over the image and is built upon the Resnet-50 architecture. We report the mean accuracy and standard deviation over 3 runs. The network is trained from scratch and the data augmentations are limited to random horizontal flips, random rotation and random cropping. The details on hyper-parameters to train the network are provided in the supplementary document.

4.1.1 Results

Figure 2 lists the relative accuracies w.r.t $\mathcal{D}_C$ for different stylisations($\frac{\mathcal{D}_G}{\mathcal{D}_C}$ and $\frac{\mathcal{D}_I}{\mathcal{D}_C}$). When comparing Acc($\mathcal{D}_C$) with corresponding $\mathcal{D}_I$ and $\mathcal{D}_G$, we observe significant drop in performance. We can also see the varying nature of the gaps in performance across the datasets. This shows that the colours do influence a network but in varying degree. Moreover, for STL-10 and Oxofrd-IIIT Pets, if we compare Acc($\mathcal{D}_C$) to Acc($\mathcal{D}_G$) we observe that the drop in accuracy is there but comparatively less than the other datasets. This suggests that the network also relies on non-colour features (such as local shapes, textures) to make a decision. Additionally, by comparing Acc($\mathcal{D}_G$) and Acc($\mathcal{D}_I$) we can notice the consistently lower performance for the latter. This suggests that incorrect colour information does indeed harm the prediction accuracy.

These results indicate that even though a CNN can represent local shape [29] or is biased towards texture[11], colours plays an important part at a local setting.

[1] Sourced from official github implementation

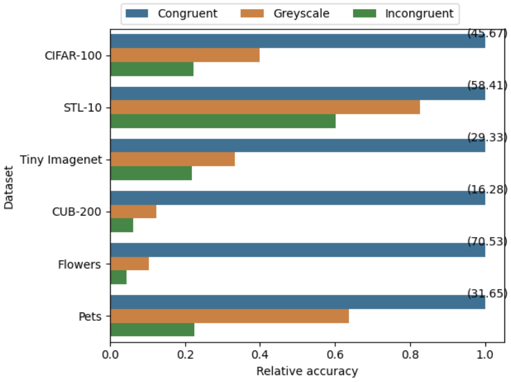

Figure 2: Performance of BagNet-9 on different test stylisations

4.2 Access to global information

In the previous experiment, we limited the view of the network to only attend to 9×9 patches of the image in a global shape agnostic fashion. Here, we use ResNet-18 which has no such restriction on its receptive field. It can thus tend to global shape information in the image.

To assess the importance of colours we train a network in the following 4 ways:

1. **Vanilla training**: Similar to the setting in Section 4.1, we train the network from scratch. The data augmentations used are random rotation, random cropping and random horizontal flips.
2. **Fine-tuning**: In practice, often an ImageNet [33] pre-trained network is fine tuned on the dataset at hand [43]. In this experiment, we follow this protocol keeping the augmentation strategy identical to vanilla training.
3. **Fine-tuning with Augmentations**:
   - **Colour augmentation**: Often colour based augmentations are used in training [44, 45] allowing the network to be colour invariant. All the training settings are identical to fine-tune except for the fact that we also add random colour jitter (hue, saturation, contrast, and brightness) to an image while training.
   - **Channel switch pre-training**: Many of the previous works studying the shape and texture bias have imposed learning limitations by first training the network on stylised data [10, 11] and then fine-tuning on original images. This has been shown to improve predictive performance of the model. Following this approach, we first start with an ImageNet pre-trained model (on congruent images). Then we fine-tune the network following 'colour augmentation' protocol with *randomised channel switching* as an additional data augmentation method. We do this in order to emulate stylised pre-training[11]. After fine-tuning the model, we disable the colour augmentations ('colour jitter' and 'randomised channel switching') and fine-tune the network further only on congruent images.

All the hyper-parameter details are provided in the appendix (see Appendix A.4). We also provide vanilla training results for MobileNet-v2 and DenseNet-121 alongside ResNet-18 and BagNet-9 (see Appendix 4.3).

4.2.1 Results & Observations

The results are shown in figure 3. Detailed results are available in the appendix (see appendix A.3). We can draw the following observations from the results.

1. For vanilla and fine-tuned networks, $Acc(\mathcal{D}_C^{test}) > Acc(\mathcal{D}_G^{test}) > Acc(\mathcal{D}_I^{test})$. This trend is similar to what existing studies report for object recognition by humans[9, 35]. However, the difference in CNN accuracies across stylisations are significantly larger. Apart from scoring human participants solely based on accuracy, their response time is also taken into account. For a CNN, there is no variation in the inference time as the architecture remains

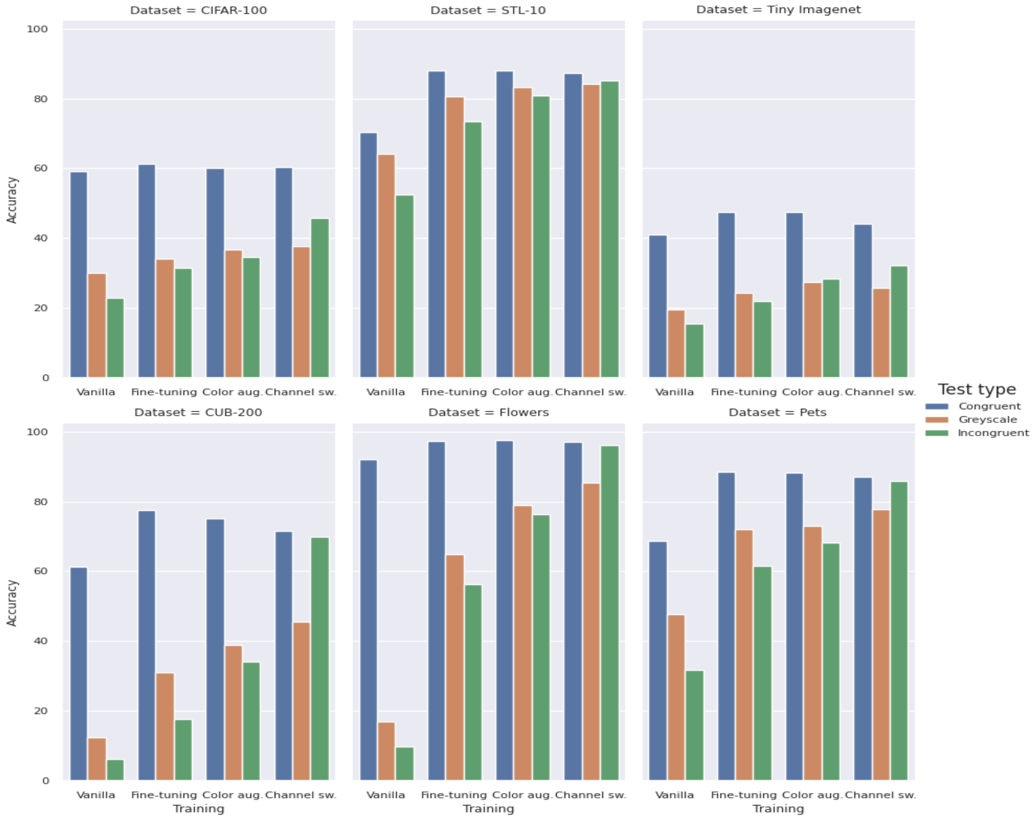

Figure 3: Top-1 $\mathcal{D}^{test}$ accuracies for different training strategies.

constant. However, it can be an interesting extension to understand the differences arising over the predicted estimate. For instance, many approaches utilise predicted value for the winning category as a network's confidence in its prediction [46]. The aim of the study will be then to observe the potential impact of colours on its confidence estimate.

2. Fine-tuning a pre-trained model is widely known to improve the learnt representations of a model and subsequently its accuracy. We observe the additional benefit of fine-tuning which leads to better performance for greyscale and incongruent images indicating lower dependency on colours.

3. Incorporating colour augmentations and channel-switching into training can enforce a model to further rely less on colours. But, it does not improve the network's accuracy for congruent images.

4. The variability for cross-style performance is high across datasets. For example, in the vanilla training setting CUB-200 shows a significantly low performance for greyscale when compared to Oxford-IIIT Pets. We make a similar observation when comparing STL-10 with CIFAR-100. One common property of STL-10 and Pets is that they consist of relatively smaller number of classes (10 and 37 respectively) when compared to CIFAR-100 and CUB-200 (100 and 200 respectively). A direction for future work can be to investigate the relationship between number of categories in the dataset and colour dependency of a CNN. Apart from exploring the dependency over the number of categories we can also investigate if this variation is dependent on categories in the dataset. As humans, we rely more on colours for recognising natural objects than man-made objects [6]. This property is referred to as colour diagnosticity. A similar observation if it exists for CNNs can be worth exploring.

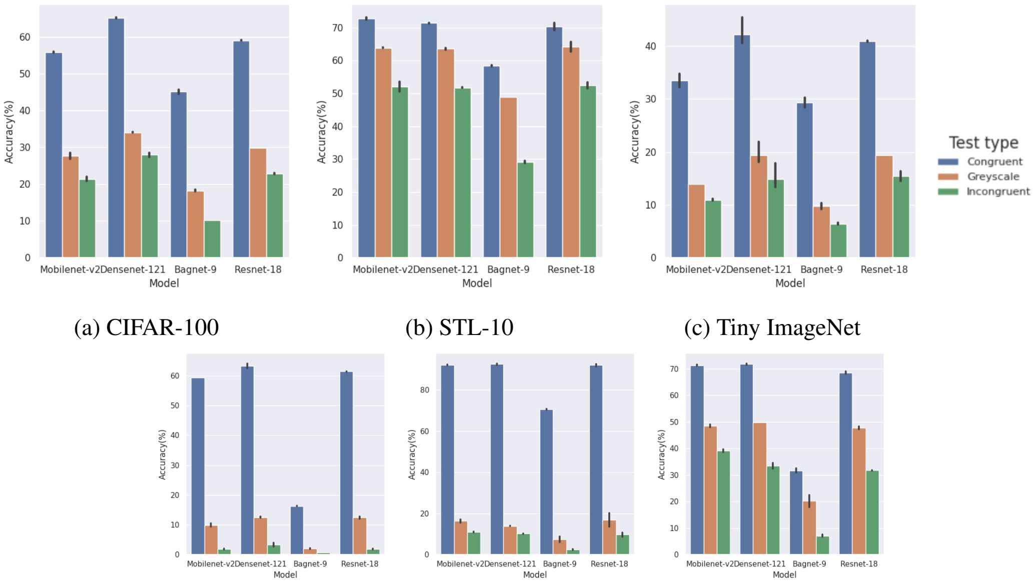

(a) CIFAR-100 (b) STL-10 (c) Tiny ImageNet

(d) CUB-200-2011 (e) Oxford-Flowers (f) Oxford-IIIT Pets

Figure 4: Vanilla training results for different architectures

4.3 Vanilla Performance Across Architectures

In this experiment we include MobileNet-v2 [47] and DenseNet-121 [48] along with ResNet-18 and BagNet-9 to compare their performance across different datasets. This way we can examine if architectural differences play a role in colour bias.
We report the results on different CNN architectures trained under the vanilla setting in Figure 4. The results show that different architectures display similar behaviour for colour importance across datasets. On the congruent images, the networks perform the best whereas the performance is worst for incongruent images. This shows that the underlying the architecture plays a less significant role in driving the bias of a network towards colour. The importance of colour is more dependent on the task at hand.

5 Conclusion

We believe ours is the first work to recognise unattributed impact of colours to the shape/texture driven research for understanding bias in CNNs. By adopting the psychophysical experiment for CNNs, we have provided empirical evidence to highlight high impact of colours. We showed that a variety of different CNNs show high colour dependency for the classification task. This dependency appears to be tied to the dataset than the underlying architecture. By default, the networks are highly colour dependent and this dependency can be reduced by utilizing pre-trained weights and employing various augmentations in training as showed in our work.

References

[1] Inês Bramão, Luís Faísca, Karl Magnus Petersson, and Alexandra Reis. The contribution of color to object recognition. In Ioannis Kypraios, editor, *Advances in Object Recognition Systems*, chapter 4. IntechOpen, Rijeka, 2012. doi: 10.5772/34821. URL `https://doi.org/10.5772/34821`.

[2] Aave Hannus, Ronald van den Berg, Harold Bekkering, Jos B. T. M. Roerdink, and Frans W. Cornelissen. Visual search near threshold: Some features are more equal than others. *Journal of Vision*, 6(4):15–15, 07 2006. ISSN 1534-7362. doi: 10.1167/6.4.15. URL `https://doi.org/10.1167/6.4.15`.

[3] Antje Nuthmann and George L. Malcolm. Eye guidance during real-world scene search: The role color plays in central and peripheral vision. *Journal of Vision*, 16(2):3–3, 01 2016. ISSN 1534-7362. doi: 10.1167/16.2.3. URL `https://doi.org/10.1167/16.2.3`.

[4] Irving Biederman and Ginny Ju. Surface versus edge-based determinants of visual recognition. *Cognitive Psychology*, 20(1):38 – 64, 1988. ISSN 0010-0285. doi: https://doi.org/10.1016/0010-0285(88)90024-2. URL `http://www.sciencedirect.com/science/article/pii/0010028588900242`.

[5] Irving Biederman. Recognition-by-components: a theory of human image understanding. *Psychological review*, 94 2:115–147, 1987.

[6] James W. Tanaka and Lynn M. Presnell. Color diagnosticity in object recognition. *Perception & Psychophysics*, 61(6):1140–1153, Aug 1999. ISSN 1532-5962. doi: 10.3758/BF03207619. URL `https://doi.org/10.3758/BF03207619`.

[7] Galit Naor-Raz, Michael J Tarr, and Daniel Kersten. Is color an intrinsic property of object representation? *Perception*, 32(6):667–680, 2003. doi: 10.1068/p5050. URL `https://doi.org/10.1068/p5050`. PMID: 12892428.

[8] J. R. Stroop. Studies of interference in serial verbal reactions. *Journal of Experimental Psychology*, 18(6):643–662, 1935. ISSN 0022-1015(Print). doi: 10.1037/h0054651. URL `https://doi.org/10.1037/h0054651`.

[9] Simen Hagen, Quoc C. Vuong, Lisa S. Scott, Tim Curran, and James W. Tanaka. The role of color in expert object recognition. *Journal of Vision*, 14(9):9–9, 08 2014. ISSN 1534-7362. doi: 10.1167/14.9.9. URL `https://doi.org/10.1167/14.9.9`.

[10] Hossein Hosseini, Baicen Xiao, Mayoore Jaiswal, and Radha Poovendran. Assessing shape bias property of convolutional neural networks. In *The IEEE Conference on Computer Vision and Pattern Recognition (CVPR) Workshops*, June 2018.

[11] Robert Geirhos, Patricia Rubisch, Claudio Michaelis, Matthias Bethge, Felix A Wichmann, and Wieland Brendel. Imagenet-trained CNNs are biased towards texture; increasing shape bias improves accuracy and robustness. In *International Conference on Learning Representations*, 2019. URL `https://openreview.net/forum?id=Bygh9j09KX`.

[12] Jürgen Schmidhuber. Deep learning in neural networks: An overview. *Neural Networks*, 61: 85 – 117, 2015. ISSN 0893-6080. doi: https://doi.org/10.1016/j.neunet.2014.09.003. URL `http://www.sciencedirect.com/science/article/pii/S0893608014002135`.

[13] O. Abdel-Hamid, A. Mohamed, H. Jiang, L. Deng, G. Penn, and D. Yu. Convolutional neural networks for speech recognition. *IEEE/ACM Transactions on Audio, Speech, and Language Processing*, 22(10):1533–1545, 2014.

[14] Yoav Goldberg. Neural network methods for natural language processing. *Synthesis Lectures on Human Language Technologies*, 10(1):1–309, 2017. doi: 10.2200/S00762ED1V01Y201703HLT037. URL `https://doi.org/10.2200/S00762ED1V01Y201703HLT037`.

[15] Chenyi Chen, Ari Seff, Alain Kornhauser, and Jianxiong Xiao. Deepdriving: Learning affordance for direct perception in autonomous driving. In *The IEEE International Conference on Computer Vision (ICCV)*, December 2015.

[16] Matthew D. Zeiler and Rob Fergus. Visualizing and understanding convolutional networks. In David Fleet, Tomas Pajdla, Bernt Schiele, and Tinne Tuytelaars, editors, *Computer Vision – ECCV 2014*, pages 818–833, Cham, 2014. Springer International Publishing. ISBN 978-3-319-10590-1.

[17] Grégoire Montavon, Wojciech Samek, and Klaus-Robert Müller. Methods for interpreting and understanding deep neural networks. *Digital Signal Processing*, 73:1 – 15, 2018. ISSN 1051-2004. doi: https://doi.org/10.1016/j.dsp.2017.10.011. URL `http://www.sciencedirect.com/science/article/pii/S1051200417302385`.

[18] Christian Szegedy, Wojciech Zaremba, Ilya Sutskever, Joan Bruna, Dumitru Erhan, Ian Goodfellow, and Rob Fergus. Intriguing properties of neural networks. In *International Conference on Learning Representations*, 2014. URL `http://arxiv.org/abs/1312.6199`.

[19] Karen Simonyan, Andrea Vedaldi, and Andrew Zisserman. Deep inside convolutional networks: Visualising image classification models and saliency maps. In *Workshop at International Conference on Learning Representations*, 2014.

[20] M. Engilberge, E. Collins, and S. Süsstrunk. Color representation in deep neural networks. In *2017 IEEE International Conference on Image Processing (ICIP)*, pages 2786–2790, 2017.

[21] Jonas Kubilius, Stefania Bracci, and Hans P. Op de Beeck. Deep neural networks as a computational model for human shape sensitivity. *PLOS Computational Biology*, 12(4):1–26, 04 2016. doi: 10.1371/journal.pcbi.1004896. URL `https://doi.org/10.1371/journal.pcbi.1004896`.

[22] Astrid A. Zeman, J. Brendan Ritchie, Stefania Bracci, and Hans Op de Beeck. Orthogonal representations of object shape and category in deep convolutional neural networks and human visual cortex. *Scientific Reports*, 10(1):2453, Feb 2020. ISSN 2045-2322. doi: 10.1038/s41598-020-59175-0. URL `https://doi.org/10.1038/s41598-020-59175-0`.

[23] Samuel Ritter, David G. T. Barrett, Adam Santoro, and Matthew M Botvinick. Cognitive psychology for deep neural networks: A shape bias case study. *ArXiv*, abs/1706.08606, 2017.

[24] Reuben Feinman and Brenden M. Lake. Learning inductive biases with simple neural networks. *ArXiv*, abs/1802.02745, 2018.

[25] Kamila M. Jozwik, Nikolaus Kriegeskorte, Katherine R. Storrs, and Marieke Mur. Deep convolutional neural networks outperform feature-based but not categorical models in explaining object similarity judgments. *Frontiers in Psychology*, 8:1726, 2017. ISSN 1664-1078. doi: 10.3389/fpsyg.2017.01726. URL `https://www.frontiersin.org/article/10.3389/fpsyg.2017.01726`.

[26] Gaurav Malhotra and Jeff Bowers. The contrasting roles of shape in human vision and convolutional neural networks. In *CogSci*, 2019.

[27] Katherine L. Hermann and Simon Kornblith. Exploring the origins and prevalence of texture bias in convolutional neural networks, 2019.

[28] Wieland Brendel and Matthias Bethge. Approximating cnns with bag-of-local-features models works surprisingly well on imagenet. *International Conference on Learning Representations*, 2019. URL `https://openreview.net/pdf?id=SkfMWhAqYQ`.

[29] Nicholas Baker, Hongjing Lu, Gennady Erlikhman, and Philip J. Kellman. Deep convolutional networks do not classify based on global object shape. *PLOS Computational Biology*, 14 (12):1–43, 12 2018. doi: 10.1371/journal.pcbi.1006613. URL `https://doi.org/10.1371/journal.pcbi.1006613`.

[30] Mihran Tuceryan and Anil K. Jain. *Texture Analysis*, page 235–276. World Scientific Publishing Co., Inc., USA, 1993. ISBN 9810211368.

[31] R. M. Haralick. Statistical and structural approaches to texture. *Proceedings of the IEEE*, 67(5): 786–804, 1979.

[32] Leon A. Gatys, Alexander S. Ecker, and Matthias Bethge. Texture synthesis using convolutional neural networks. In *Proceedings of the 28th International Conference on Neural Information Processing Systems - Volume 1*, NIPS'15, page 262–270, Cambridge, MA, USA, 2015. MIT Press.

[33] J. Deng, W. Dong, R. Socher, L.-J. Li, K. Li, and L. Fei-Fei. ImageNet: A Large-Scale Hierarchical Image Database. In *CVPR09*, 2009.

[34] Hyojin Bahng, Sanghyuk Chun, Sangdoo Yun, Jaegul Choo, and Seong Joon Oh. Learning de-biased representations with biased representations, 2019.

[35] David J. Therriault, Richard H. Yaxley, and Rolf A. Zwaan. The role of color diagnosticity in object recognition and representation. *Cognitive Processing*, 10:335–342, 2009.

[36] Alex Krizhevsky. Learning multiple layers of features from tiny images. Technical report, 2009.

[37] Adam Coates, Andrew Ng, and Honglak Lee. An analysis of single-layer networks in unsupervised feature learning. In *Proceedings of the Fourteenth International Conference on Artificial Intelligence and Statistics*, Proceedings of Machine Learning Research, pages 215–223. PMLR, 2011. URL `http://proceedings.mlr.press/v15/coates11a.html`.

[38] Olga Russakovsky, Jia Deng, Hao Su, Jonathan Krause, Sanjeev Satheesh, Sean Ma, Zhiheng Huang, Andrej Karpathy, Aditya Khosla, Michael Bernstein, Alexander C. Berg, and Li Fei-Fei. ImageNet Large Scale Visual Recognition Challenge. *International Journal of Computer Vision (IJCV)*, 115(3):211–252, 2015.

[39] P. Welinder, S. Branson, T. Mita, C. Wah, F. Schroff, S. Belongie, and P. Perona. Caltech-UCSD Birds 200. Technical report, California Institute of Technology, 2010.

[40] Maria-Elena Nilsback and Andrew Zisserman. A visual vocabulary for flower classification. In *IEEE Conference on Computer Vision and Pattern Recognition*, volume 2, pages 1447–1454, 2006.

[41] Omkar M. Parkhi, Andrea Vedaldi, Andrew Zisserman, and C. V. Jawahar. Cats and dogs. In *IEEE Conference on Computer Vision and Pattern Recognition*, 2012.

[42] B. Fuglede and F. Topsoe. Jensen-shannon divergence and hilbert space embedding. In *International Symposium onInformation Theory, 2004. ISIT 2004. Proceedings.*, pages 31–, 2004.

[43] Jason Yosinski, Jeff Clune, Yoshua Bengio, and Hod Lipson. How transferable are features in deep neural networks? In Z. Ghahramani, M. Welling, C. Cortes, N. D. Lawrence, and K. Q. Weinberger, editors, *Advances in Neural Information Processing Systems 27*, pages 3320–3328. Curran Associates, Inc., 2014. URL `http://papers.nips.cc/paper/5347-how-transferable-are-features-in-deep-neural-networks.pdf`.

[44] Andrew G. Howard. Some improvements on deep convolutional neural network based image classification. *CoRR*, abs/1312.5402, 2014.

[45] C. Szegedy, Wei Liu, Yangqing Jia, P. Sermanet, S. Reed, D. Anguelov, D. Erhan, V. Vanhoucke, and A. Rabinovich. Going deeper with convolutions. In *2015 IEEE Conference on Computer Vision and Pattern Recognition (CVPR)*, pages 1–9, 2015.

[46] Chuan Guo, Geoff Pleiss, Yu Sun, and Kilian Q. Weinberger. On calibration of modern neural networks, 2017.

[47] M. Sandler, A. Howard, M. Zhu, A. Zhmoginov, and L. Chen. Mobilenetv2: Inverted residuals and linear bottlenecks. In *2018 IEEE/CVF Conference on Computer Vision and Pattern Recognition*, pages 4510–4520, June 2018. doi: 10.1109/CVPR.2018.00474. URL `https://ieeexplore.ieee.org/document/8578572`.

[48] Gao Huang, Zhuang Liu, Laurens van der Maaten, and Kilian Q Weinberger. Densely connected convolutional networks. In *Proceedings of the IEEE Conference on Computer Vision and Pattern Recognition*, 2017.

A Appendix

A.1 Data

Category	Dataset	#Classes	$\|\mathcal{D}^{train}\|$	$\|\mathcal{D}^{test}\|$	Image size
Image classification	CIFAR-100[36]	100	$50,000$	$10,000$	32×32
	STL-10[37]	10	$5,000$	$8,000$	96×96
	Tiny ImageNet[38]	200	$100,000$	$5,000$	64×64
Fine-Grained Visual Classification	CUB-200[39]	200	$5,994$	$5,794$	224×224
	Oxford-Flowers[40] [2]	102	$6,149$	$2,040$	224×224
	Oxford-IIIT Pets[41]	37	$3,680$	$3,669$	224×224

Table 1: Dataset statistics

A.2 Jensen-Shannon Measure

To reiterate the notations used, a dataset $\mathcal{D} = \{(x_i, y_i), i = 1, \ldots, N\}$ is composed of images $x_i \in \mathbb{R}^{C \times H \times W}$ and their corresponding labels y_i. $\mathcal{D}^{train}$, $\mathcal{D}^{test}$ denotes the split of the dataset into train and test sets respectively. Jensen Shannon divergence between two stylisations of the same dataset is defined as:

$$JS(\mathcal{D}_1^{train}, \mathcal{D}_2^{train}) = \frac{1}{|\mathcal{D}^{train}|} \sum_{i \in \mathcal{D}^{train}} \frac{1}{|C|} \sum_{j \in C} JS(T_1(x_i)[j], T_2(x_i)[j])$$

where, T_i is the transformation corresponding to $\mathcal{D}_i$ and indexing $[j]$ returns the normalised intensity histogram for the j^{th} channel.

The corresponding results in Table 2 show that switching channels is a gentler transformation than composing negatives in preserving original shape and texture. Greyscale is consistently with the least amount of JS divergence and can suggest as to why consistently Acc($\mathcal{D}_G$) > Acc($\mathcal{D}_I$).

Table 2: JS measure between stylisations

Datasets	$JS(\mathcal{D}_C^{train}, \mathcal{D}_G^{train})$	$JS(\mathcal{D}_C^{train}, \mathcal{D}_I^{train})$	$JS(\mathcal{D}_C^{train}, \mathcal{D}_{Neg}^{train})$
CIFAR-100	0.07	0.12	0.33
Tiny ImageNet	0.06	0.1	0.29
STL10	0.06	0.1	0.3
CUB-200	0.1	0.15	0.34
Oxford-Flowers	0.09	0.13	0.32
Oxford-IIIT Pets	0.04	0.07	0.27

A.3 Detailed Test results

A.4 Training details

We utilised Pytorch framework for all of our experiments. We list the detailed hyper-parameters below. Missing key-values in table i can be found via. recursive search in table $i - 1$. All the fine-grained datasets utilise similar training hyper-parameters and hence we have provided only the details for CUB-200.

Table 3:
Test accuracies(in %) for different training strategies on classification datasets.

Training approach	Datasets	Acc($\mathcal{D}_C$)	Acc($\mathcal{D}_G$)	Acc($\mathcal{D}_I$)
Vanilla	CIFAR-100	59.10 ± 0.11	29.90 ± 0.03	22.86 ± 0.16
	STL-10	70.30 ± 1.67	64.13 ± 2.13	52.47 ± 1.29
	STL-10	40.88 ± 0.10	19.40 ± 0.02	15.47 ± 1.31
Fine-tuning	CIFAR-100	$\mathbf{61.39} \pm 0.12$	34.13 ± 0.16	31.53 ± 0.55
	STL-10	$\mathbf{88.10} \pm 0.30$	80.59 ± 0.39	73.45 ± 0.69
	STL-10	$\mathbf{47.52} \pm 0.09$	24.38 ± 0.21	21.96 ± 0.19
Colour augmentation	CIFAR-100	60.06 ± 0.29	36.68 ± 0.82	34.67 ± 0.24
	STL-10	88.04 ± 0.23	83.29 ± 0.46	80.88 ± 0.06
	STL-10	47.42 ± 0.39	$\mathbf{27.41} \pm 1.10$	28.27 ± 0.09
Channel switch pre-training	CIFAR-100	60.24 ± 0.22	$\mathbf{37.76} \pm 0.26$	$\mathbf{45.84} \pm 0.44$
	STL-10	87.20 ± 0.45	$\mathbf{84.01} \pm 0.19$	$\mathbf{85.23} \pm 0.21$
	Tiny Imagenet	44.20 ± 0.16	25.75 ± 0.46	$\mathbf{32.11} \pm 0.02$

Table 4:
Test accuracies(in %) for different training strategies on fine-grained datasets.

Training approach	Datasets	Acc($\mathcal{D}_C$)	Acc($\mathcal{D}_G$)	Acc($\mathcal{D}_I$)
Vanilla	CUB	61.39 ± 0.03	12.40 ± 0.58	6.03 ± 0.23
	Oxford-Flowers	92.03 ± 0.72	16.88 ± 4.81	9.68 ± 1.42
	OP	68.61 ± 0.63	47.75 ± 0.80	31.77 ± 0.15
Fine-tuning	CUB	$\mathbf{77.39} \pm 0.40$	30.99 ± 0.36	17.62 ± 2.30
	Oxford-Flowers	97.37 ± 0.03	64.77 ± 1.42	56.27 ± 3.32
	OP	$\mathbf{88.51} \pm 0.86$	72.06 ± 1.15	61.59 ± 2.11
Colour augmentation	CUB	75.07 ± 0.09	38.85 ± 1.33	34.09 ± 0.15
	Oxford-Flowers	$\mathbf{97.50} \pm 0.14$	78.82 ± 0.67	76.37 ± 1.82
	Pets	88.15 ± 0.32	72.86 ± 0.05	68.22 ± 1.04
Channel switch pre-training	CUB	71.5 ± 0.67	$\mathbf{45.41} \pm 0.32$	$\mathbf{69.93} \pm 0.57$
	Oxford-Flowers	97.15 ± 0.06	$\mathbf{85.44} \pm 1.24$	$\mathbf{96.17} \pm 0.21$
	OP	87.16 ± 1.04	$\mathbf{77.65} \pm 1.29$	$\mathbf{85.77} \pm 1.11$

Table 5: Training details for CIFAR-100

Approach	Key	Value
Common	Models	Bagnet-9, Resnet-18, Densenet-121, Mobilenet-v2
	Image size	32×32
	Train aug.	Random(rotation, horizontal flip), standardisation
	Test aug.	Standardisation
	Batch size	128
	Optimiser	SGD
	LR decay rate	0.5
Vanilla	Epochs	200
	LR	0.1
	Train aug.	Common
	LR decay epochs	$[50, 100, 150]$
Fine-tuning	Pre-trained weights	ImageNet
	LR	0.01
	Epochs	30
	LR decay epochs	$[15]$
Colour augmentation	Pre-trained weights	ImageNet
	Train aug.	Common + Random colour jitters
	LR	0.01
	Epochs	30
	LR decay epochs	$[15]$
Incongruent Training	Pre-trained weights	ImageNet
	Train aug.	Common + Random (colour jitters, channel switching)
	Finetuned with	Random(rotation, horizontal flip)
	LR	0.01
	Epochs	$30, 30$
	LR decay epochs	$[15], [15]$

Table 6: Training details for STL-10

Approach	Element	Value
Common	Image size	96×96
	Batch size	64
Vanilla	Epochs	200
	LR	0.1
	LR decay epochs	$[40, 80, 120, 160]$
Fine-tuning	Epochs	50
	LR	0.01
	LR decay epochs	$[15, 30, 45]$
Colour augmentation	Epochs	50
	LR	0.01
	LR decay epochs	$[15, 30, 45]$
Incongruent Training	Epochs	$50, 50$
	LR	0.01
	LR decay epochs	$[15, 30, 45], [15, 30, 45]$

Table 7: Training details for Tiny ImageNet

Approach	Element	Value
Common	Image size Batch size	64×64 128
Vanilla	Epochs LR LR decay epochs	150 0.1 $[30, 60, 90, 120]$
Fine-tuning	Epochs LR LR decay epochs	50 0.01 $[15, 30, 45]$
Colour augmentation	Epochs LR LR decay epochs	50 0.01 $[15, 30, 45]$
Incongruent Training	Epochs LR LR decay epochs	$50, 50$ 0.01 $[15, 30, 45], [15, 30, 45]$

Table 8: Training details for CUB-200

Approach	Key	Value
Common	Image size Train aug. Test aug. Batch size Optimiser LR decay rate	224×224 Random(rotation, horizontal flip, crop), standardisation center crop(224), standardisation 32 SGD 0.5
Vanilla	Epochs LR Train aug. LR decay epochs	200 0.1 Common $[50, 100, 150]$
Fine-tuning	Pre-trained weights LR Train aug. Epochs LR decay epochs	ImageNet 0.01 Common 40 $[15, 30]$
Colour augmentation	Pre-trained weights LR Train aug. Epochs LR decay epochs	ImageNet 0.01 Common + Random colour jitters 40 $[15, 30]$
Incongruent Training	Pre-trained weights Train aug. Finetuned with LR Epochs LR decay epochs	ImageNet Common + Random (colour jitters, channel switching) Common aug. 0.01 $40, 40$ $[15, 30], [15, 30]$